NASA TN D-1242

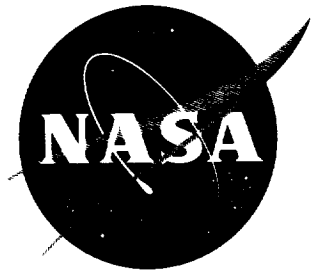

TECHNICAL NOTE

D-1242

THEORETICAL INVESTIGATION OF EFFECTS OF CHANGES IN COMMAND COMPUTATIONS AND FILTER LOCATION ON RESPONSE OF AN AUTOMATICALLY CONTROLLED INTERCEPTOR DURING THE ATTACK PHASE

By Windsor L. Sherman

Langley Research Center
Langley Station, Hampton, Va.

NATIONAL AERONAUTICS AND SPACE ADMINISTRATION

WASHINGTON May 1962

NATIONAL AERONAUTICS AND SPACE ADMINISTRATION

TECHNICAL NOTE D-1242

THEORETICAL INVESTIGATION OF EFFECTS OF CHANGES IN COMMAND COMPUTATIONS AND FILTER LOCATION ON RESPONSE OF AN AUTOMATICALLY CONTROLLED INTERCEPTOR DURING THE ATTACK PHASE

By Windsor L. Sherman

SUMMARY

Results of a study of the effects of command formulation and filter location on the response of an automatically controlled interceptor making an attack at supersonic speed on a supersonic target are reported. Large rolling oscillations occurring in the last half of the attack are eliminated by proper command formulation and filter location. Simplification of the command computation and filter are achieved without deterioration of the interceptor and system responses. The effects of radar noise are neglected.

The results, which should, in general, be applicable to radar-controlled bank-to-turn automatic control systems, are reported as time histories of the interceptor motion.

INTRODUCTION

One means of defense against piloted and pilotless bomber aircraft is the manned interceptor. These interceptors are equipped with automatic fire and flight control systems which when tied together make the interceptor mission automatic.

The mission of the interceptor may be divided into three phases: the flight to the target area, the attack, and the return to base. Research on the attack phase of the automatic interception of bombers has been reported in references 1 and 2 for a supersonic interceptor armed with unguided rockets and attacking a supersonic bomber. Reference 1 discusses the flight maneuvers of the interceptor and the manner in which the response of the interceptor was affected by nonlinear aerodynamic characteristics and the effect of nonlinear dynamics terms to determine an accurate mathematical representation of the

interceptor. Reference 2 presents the effects of different changes in the method of filtering fire-control data, computing the roll command, and limiting the normal acceleration, and also effects of gross changes in automatic pilot gains on the interceptor response. Both of these investigations were performed concurrently on a large analog computer. The results obtained in these studies indicated that large lateral oscillations, particularly in roll when a nonaccelerating target is attacked, were present in the interceptor response during the final two-thirds of the attack run. In these studies the roll control system directed the normal component of the interceptor acceleration vector at the target.

The purpose of the present study, which was performed on a large high-speed digital computer, was to investigate the effects of changes in airplane command computation and filter location on the lateral oscillations of the interceptor. It was assumed that an interceptor flying at a Mach number of 2.2 was attacking a bomber flying initially at a Mach number of 1.4 at 50,000 feet. The attack was made against a straight flying target under lead collision guidance with an assumed interceptor armament of unguided rockets.

It should be noted that the interceptor system discussed herein does not represent the current state of development of interceptor systems in that unguided rockets are used instead of guided missiles and the filter used is not as sophisticated as some proposed filters. This system was retained for this study inasmuch as the material presented herein together with that of references 1 and 2 represents a set of coherent investigations into the problems associated with a given automatic attack system for the interceptor problem.

Results of this investigation are presented as time histories of the interceptor motion during the attack run and should, in general, be applicable to radar-controlled bank-to-turn automatic control systems.

SYMBOLS

c	speed of sound
E_a, E_e	unfiltered azimuth and elevation steering errors
g	acceleration of gravity
H_t	target altitude
i, j, k	unit vectors

K	conversion factor
K_3, K_4, K_6	constants
M_a, M_e	azimuth and elevation miss distances in airplane principal body axes
$\vec{M}_d$	miss distance, $\vec{i}(0) + \vec{j}M_a + \vec{k}M_e$
m_3, n_3	direction cosines between space axes and airplane principal body axes
p, q, r	airplane rolling, pitching, and yawing velocity about X_b-, Y_b-, and Z_b-axis, respectively
R	range
R_f	future range
t	time
t_g	time to go (time from present to firing point)
u, v, w	component of interceptor velocity along X_b-, Y_b-, and Z_b-axis, respectively
$\vec{V}_f$	interceptor velocity
$\vec{V}_m$	missile velocity relative to interceptor
$\vec{V}_R$	relative velocity of interceptor and target as read by radar
$\vec{V}_T$	target velocity
X, Y, Z	right-hand Cartesian coordinate system
γ	flight-path angle
$\delta_a, \delta_e, \delta_r$	aileron, elevator, and rudder deflection angles
ϵ_a, ϵ_e	filtered azimuth and elevation steering errors in body axes
$\bar{\epsilon}_e$	flight-path command with gravity accelerations included

$\hat{\epsilon}_e$	g-limited flight-path command
θ,ϕ,ψ	Euler angles (interceptor pitch, roll (or bank), and yaw)
θ_a,θ_e	azimuth and elevation radar gimbal angles
τ	time of flight of rocket
τ_F	filter time constant
$\tau_{S,A}$	aileron servomotor time constant
$\tau_{S,E}$	elevator servomotor time constant
ϕ_c	roll command without gravity accelerations included
ϕ_c'	roll command with gravity accelerations included
$\vec{\omega}_A$	angular velocity vector of airplane, $\vec{i}p + \vec{j}q + \vec{k}r$
$\vec{\omega}_D$	angular velocity vector of radar dish, $\vec{i}(0) + \vec{j}\dot{\theta}_e + \vec{k}\dot{\theta}_a$

Subscripts:

b	principal body axes
F	filtered or smoothed variables
o	initial condition
s	space coordinate system

A dot over a symbol indicates differentiation with respect to time. An arrow over a symbol indicates a vector.

DESCRIPTION OF INTERCEPTOR SYSTEM AND COMPUTER PROGRAM

Description of Interceptor System

Figure 1(a) is a generalized block diagram of the attack-phase control of the basic interceptor system used in this study. It is the same interceptor system considered in references 1 and 2. As can be seen, the components of the system are target, radar, fire-control computer, command computer, filters, automatic pilot, and airplane.

Figure 2 shows the basic geometry of the attack phase of the interceptor system for lead-collision attacks. The basic vector equation of the fire-control computer may be written as

$$\vec{R} + \vec{V}_T\left(t_g + \tau\right) = \vec{V}_f t_g + \left(\vec{V}_f + \vec{V}_m\right)\tau + \vec{M}_d \qquad (1)$$

This equation states that the present range plus the distance the target travels in time $t_g + \tau$ is equal to the distance the interceptor travels in time t_g plus the distance the rocket travels in time τ. This equation is a first-order formulation of the fire-control problem and provides the basic logic that controls the interceptor system in the attack. Appendix A of reference 1 presents the details of the interceptor system based on equation (1).

Changes Made to Basic Interceptor System

During the study two changes were made to the interceptor system: (1) modification of the equations used to compute the normal acceleration and roll commands and (2) changing the filter location from the location of figure 1(a), the output side of the command computer, to that shown in figure 1(b), the input side of the fire-control computer. The first change involved changes in mathematics and did not change the system configuration; the second change permitted target information to be smoothed without involving interceptor information, as was necessary for the system of figure 1(a). The details of these changes are subsequently discussed in the text.

Computer Program

The equations of motion in appendix A of reference 1 were programed for solution on a large digital computer. The Runge-Kutta method was used with a fixed time interval of 0.01 second and a floating decimal point to integrate the differential equations of motion of the system. The output of the computer consisted of time histories of the system parameters and interceptor response during the attack run. The attack was initiated by specifying range, radar gimbal angles, velocity of the interceptor, and velocity and altitude of the target.

The condition for terminating an attack run was described by t_g, the time between the present and firing of the interceptor armament. Thus, at $t_g = 0$ the run was terminated. This was possible because rocket armament was assumed, and after release the interceptor motion did not affect rocket motion.

Initial Conditions

Inasmuch as the purpose of this study was to investigate some of the system factors affecting the roll response of the interceptor, an initial condition that placed a high demand on roll capability was desired. In order to maintain chronology the initial condition for this study should be one set of the initial conditions studied in reference 1. A review of previous results showed that initial condition III of reference 1 provided the desired characteristics. Figure 3 shows the axes systems used in the problem and in the orientation of the interceptor and target, and figure 4 presents a pictorial representation of the initial condition. The initial values of the parameters to set up the condition for this study are as follows:

$\Psi = \phi_o = 0$

$\theta_o = 0.0332$ radian

$V_{f,o} = 2,136$ ft/sec

$u_o = 2,135$ ft/sec

$v_o = 0$

$w_o = 70.52$ ft/sec

$p_o = q_o = r_o = 0$

$R_o = 60,000$ ft

$\theta_{a,o} = -0.7854$ radian

$\theta_{e,o} = 0$

$V_T = 1,359$ ft/sec $\left(V_T = i(0) + j(1,359) + k(0)\right)$

$H_T = 50,000$ ft

$c = 971$ ft/sec

The order of rotation for the Euler angles was Ψ, θ, and ϕ, which were referenced to a set of fixed space axes, and that for the gimbal angles was θ_a and θ_e, which were referenced to the body axes.

Two components of the interceptor system require that very specific initial conditions be used. These are the filters and servomotors. In

the study it was assumed that the radar had been tracking the target long enough to completely charge the filter; the initial conditions for the basic system were

$$\epsilon_a(0) = E_a(0) \qquad \dot{\epsilon}_a(0) = 0$$

$$\epsilon_e(0) = E_e(0) \qquad \dot{\epsilon}_e(0) = 0$$

and a similar assumption and initial conditions were used when the filter location was changed. For the servomotors it was specified that $\delta_a(0) = \delta_e(0) = 0$ and $\dot{\delta}_a(0) \neq 0$, $\dot{\delta}_e(0) \neq 0$ except for $\dot{\delta}_r$, the values of which are

$$\dot{\delta}_a = -\frac{K_3 \phi_c'}{\tau_{S,A}}$$

$$\dot{\delta}_e = \frac{K_6 K_4 \epsilon_e}{\tau_{S,E}}$$

$$\dot{\delta}_r = 0$$

RESULTS AND DISCUSSION

Presentation of Problem

Figure 5 shows the rolling response of the basic interceptor system during the attack run used in this investigation. The period from about 4 to 20 seconds is characterized by high positive and negative rolling velocities and steep gradients (fig. 5(a)). This violent rolling-velocity response produces large bank angles. (See fig. 5(b).) This figure gives the direction cosine m_3 which for the small pitch angles involved in this study is effectively the sine of the bank angle. In figure 6(a) it can be seen that the motions of the interceptor follow the roll command ϕ_c. Since this condition occurs in the roll command as well as in the interceptor roll response, the problem area involves, at least in part, the computation of the roll command. The roll command was computed by

$$\phi_c = \tan^{-1} \frac{\epsilon_a}{\epsilon_e}$$

The flight-path command was $\hat{\epsilon}_e$, the acceleration limited value of the vertical steering error ϵ_e. This command formulation neglects the accelerations of the earth's gravity field. The limiting was accomplished by the command g-limiter (see ref. 1), which was set for 5g and -2g. Figures 6(b) and 6(c) show the time histories of ϵ_a and ϵ_e during the run under consideration. An examination of these time histories and of that of the roll command reveals that ϵ_e approaches 0 while ϵ_a remains finite at the points where the larger bank commands occur. This result indicates that gravity accelerations should be included in the command computation, because with gravity included in the command computation the denominator of the roll command does not approach 0 until ϵ_e approaches the level of -1g. In the present formulation the roll-command denominator approaches 0 as ϵ_e approaches 0 and, thereby, adverse rolling command and motion are created.

Effect of Including Gravity Accelerations in Roll and Flight-Path Commands

If the accelerations of the gravity field are included in command formulation, the new roll command ϕ_c' is given by

$$\phi_c' = \tan^{-1} \frac{\epsilon_a - \frac{m_3 g}{K}}{\epsilon_e + \frac{n_3 g}{K}} \tag{2}$$

and the new flight-path command $\bar{\epsilon}_e$ by

$$\bar{\epsilon}_e = \left[\left(\epsilon_a - \frac{m_3 g}{K} \right)^2 + \left(\epsilon_e + \frac{n_3 g}{K} \right)^2 \right]^{1/2} - \frac{n_3 g}{K} \tag{3}$$

where the constant K is a conversion factor that makes the linear accelerations of the gravity field compatible with the angular commands ϵ_a and ϵ_e. The constant K has a nominal value of 3,150 radians/ft/sec^2. This gain is derived by considering the steady-state condition of the flight-path control loop. In the form of the roll command given by equation (2) the denominator approaches $\frac{n_3 g}{K}$

instead of 0 as ϵ_e approaches 0; the problem that occurred when ϵ_e was used by itself is thereby eliminated. In addition, this equation defines a smaller roll command as it points the resultant acceleration vector of the interceptor at the target instead of the normal component as was done by equation (1). Figures 7(a) and 7(b) show that these changes in command computation caused the roll oscillation to be more heavily damped and have slightly lower initial amplitude; however, at the firing time of 19.25 seconds the oscillation was still present but greatly improved. Figure 7(c) shows the change in flight-path response that occurred as a result of changes in the command computation. As can be seen, the last two-thirds of the time history is much less oscillatory and produces less violent changes in normal accelerations. The results of unpublished calculations indicated that this improvement was primarily due to the improvement in roll response.

L 1 5 1 8

The improvement caused by the inclusion of gravity accelerations in the roll command occurs because the command becomes singular at a different point. When gravity accelerations are omitted and no excess normal acceleration is called for, the denominator of the roll command becomes 0 for the level flight conditions of 1 g. However, when gravity accelerations are included, the zero condition does not occur until ϵ_e reaches -1 g, precluding the possibility of an oscillation from this source when the interceptor flight becomes nonaccelerated. The residual roll oscillations indicated in figures 7(a) and 7(b) therefore arise from some other cause. Figure 8 compares the roll command ϕ_c with gravity accelerations omitted and gravity accelerations included. The inclusion of gravity accelerations produces the largest effect during the last two-thirds of the time history.

Effect of Changing Filter Location

The effect of changing the filter location in the interceptor system was determined. The filter used up to the present time was the cross-roll filter; for a complete discussion, see reference 2. In this filter the angular motions of the interceptor are compensated so that they are not filtered but the linear velocities are still subject to the action of the filter. The filter was moved from the output side of the fire-control computer to the output side of the radar. (See figs. 1 and 2.) When the filter is located as shown in figure 1(b), it is referred to as the forward filter. In this location it is possible to arrange the filter so that no interceptor motions are smoothed. In actual hardware this arrangement is made as follows. Let $\vec{V}_R$ be the velocity output of the radar and $\vec{V}_f$ be the velocity of the interceptor; then

$$\vec{V}_T = \vec{V}_R + \vec{V}_f \tag{4}$$

gives the target velocity. This target velocity $\vec{V}_T$ is then fed to a cross-roll filter so that

$$\vec{V}_T = \vec{V}_{T,F} + \tau_F\left[\frac{d}{dt}\left(V_{T,F}\right) + \vec{\omega}_A \times \vec{V}_{T,F}\right] \tag{5}$$

Since $\vec{V}_T$, $\vec{V}_{T,F}$, and $\vec{\omega}_A$ are all three-component vectors, equation (5) represents a three-channel filter. The output of the filter $\vec{V}_{T,F}$ is now recombined with $\vec{V}_f$ to obtain $\vec{V}_{R,F}$ required in the fire-control computer, as follows:

$$\vec{V}_{R,F} = \vec{V}_{T,F} + \vec{V}_f \tag{6}$$

The representation of this filter in the computing program is much simpler than indicated herein inasmuch as $\vec{V}_T$ is independently available and can be fed to the filter and equation (6) can be used to obtain $\vec{V}_{R,F}$. The forward filter as defined by equation (5) was combined with the commands ϕ_c' and $\bar{\epsilon}_e$ and an attack run was computed with the standard initial condition. When the forward filter is used, the equations for the commands change slightly because of input differences. Equations (2) and (3) as presented receive the output of the rear filter ϵ_a and ϵ_e. Because of the change in filter location, E_a and E_e, the output of the fire-control computer, are substituted for the ϵ_a and ϵ_e output of the filter in equations (2) and (3); otherwise the command equations are unchanged. Figures 9(a) and 9(b) compare the rolling velocity p and the direction cosine m_3 for the forward and rear filters, both of which have the roll and pitch commands ϕ_c' and $\bar{\epsilon}_e$. The change in filter location eliminates the rolling oscillations that were present with the so-called rear filter. As the roll and pitch commands are coupled, roll causes an interchange of error between azimuth and elevation; it would be expected that with the reduced roll oscillations the normal acceleration would be smoothed. The $\dot{\gamma}$-response (vehicle is proportional to the normal acceleration) is compared for the two filters in figure 9(c); as can be seen, the smoothing of the roll response obtained with the new rear-filter location and command equations results in a smoothing of the $\dot{\gamma}$-response.

L 1 5 1 8

System Simplifications

As compared with those for the basic interceptor system, the equations for computing the commands (eqs. (2) and (3)) and the filter equation (eq. (5)) for the modified system are more complicated although as indicated in figures 7 and 9 the responses of the interceptor were considerably improved. A program of computer runs was made to determine whether equations for command computations and the filter could be simplified without sacrificing the improved response. As a result of these studies it was found that

L
1
5
1
8

(1) In computing the flight-path command, $\bar{\epsilon}_e$ (eq. (3)) could be replaced by E_e

(2) The roll command ϕ_c' could be computed by

$$\phi_c' = \frac{\epsilon_a - \frac{m_3 g}{K}}{\left| \epsilon_e + \frac{n_3 g}{K} \right|}$$

(3) The filter (eq. (5)) could be replaced by one in which the x-component of the target was unfiltered and all angular velocities except the rolling velocity p were omitted. This is the same configuration as the original filter.

Figure 10 compares the time histories of the interceptor responses for the basic system, the system incorporating gravity accelerations in the roll and flight-path commands with the three-channel forward filter, and the system simplified as previously indicated. As can be seen the introduction of these simplifications in the system considered resulted in no deterioration of the improvement obtained in roll response with the more exact equations.

While the lateral response of the airplane was the primary interest in this study, changes to the interceptor system that caused a deterioration of the final predicted miss distance, that is, the miss distance at $t_g = 0$, would not constitute acceptable modifications in spite of improved lateral response for the airplane. The following table compares the final predicted miss distances in azimuth M_a and elevation M_e for the system configurations of figure 10:

System	M_a	M_e
Basic	24	-42
Gravity accelerations included in commands and three-channel forward filter	-3.0	0.25
Simplified	-3.0	0.25

These results are for a perfect interceptor system without noise which would be present in an actual interceptor. With noise present the magnitudes of the miss distances would increase. However, the extremely low magnitude for the perfect system and the change of miss distance in the presence of noise, as developed in other studies, indicate that with noise present the miss distances could be held to acceptable magnitudes.

Other Initial Conditions and Maneuvering Targets

Primary emphasis was placed on a nonmaneuvering target and an attack condition that demanded high roll response. The simplified system was used for the other initial conditions of reference 1 and for targets making a $\pm 2g$ vertical plane maneuver. These check studies indicated that the results of this study were not modified for changes in initial conditions and target conditions.

CONCLUDING REMARKS

The basic maneuver used by the interceptor in the attack run studied was a 5g climbing turn. In this maneuver the pitch and roll commands were applied simultaneously. Large rolling oscillations that occurred in the last two-thirds of the attack run for the basic interceptor system were eliminated by (1) including gravity accelerations in the roll command and (2) moving the filter from the output side of the command computer to the input side of the fire-control computer. The flight-path command produced the same response with and without gravity accelerations.

It was found that the inverse tangent function could be replaced by its argument, if the absolute value of the denominator was used in the computation, without affecting the response of the interceptor. Similarly, it was found that the three-channel filter could be reduced to a two-channel filter with a cross-roll correction that was a function of rolling velocity.

The modifications to the basic system produced a reduction in magnitude of the final predicted miss distances which was not affected by system logic simplifications.

The results indicated that further research on the relative importance of the gravity acceleration components $m_3 g$ and $n_3 g$ in the roll command and of the filtering techniques is desirable.

Langley Research Center,
National Aeronautics and Space Administration,
Langley Air Force Base, Va., February 1, 1962.

REFERENCES

1. Sherman, Windsor L., and Schy, Albert A.: Theoretical Investigation of the Attack Phase of an Automatic Interceptor System at Supersonic Speeds With Particular Attention to Aerodynamic and Dynamic Representation of the Interceptor. NACA RM L56J08, 1957.

2. Sherman, Windsor L.: Analog Computer Study of Some Filtering, Command-Computer, and Automatic-Pilot Problems Connected With the Attack Phase of the Automatically Controlled Supersonic Interceptor. NACA RM L57G23, 1957.

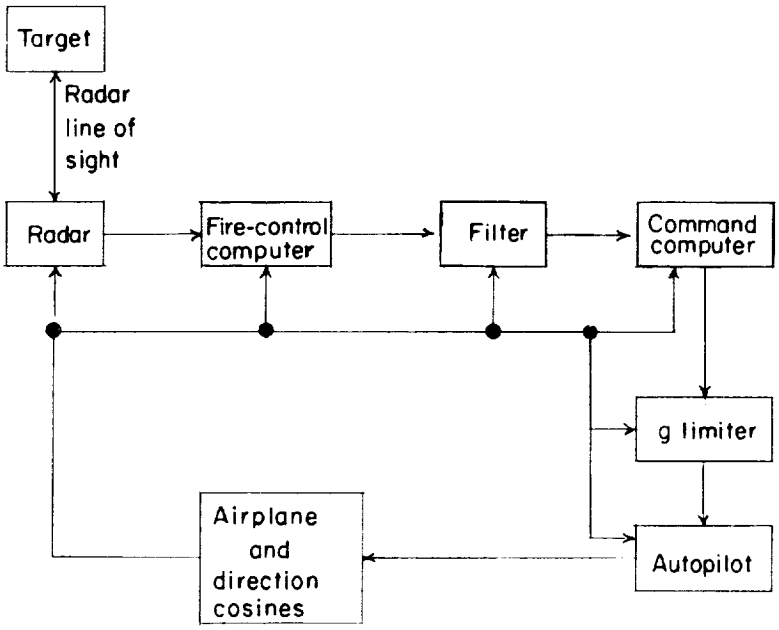

(a) Basic system.

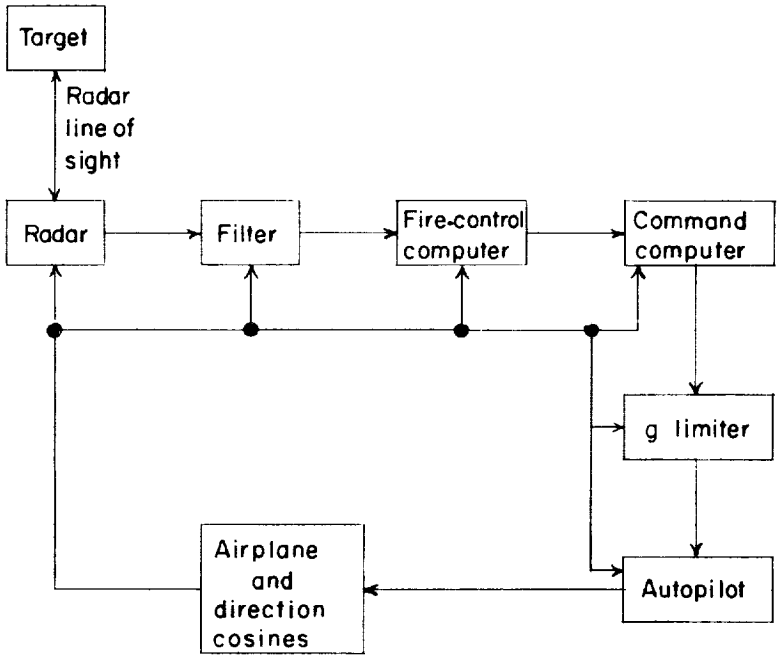

(b) Modified system.

Figure 1.- Block diagrams of interceptor system.

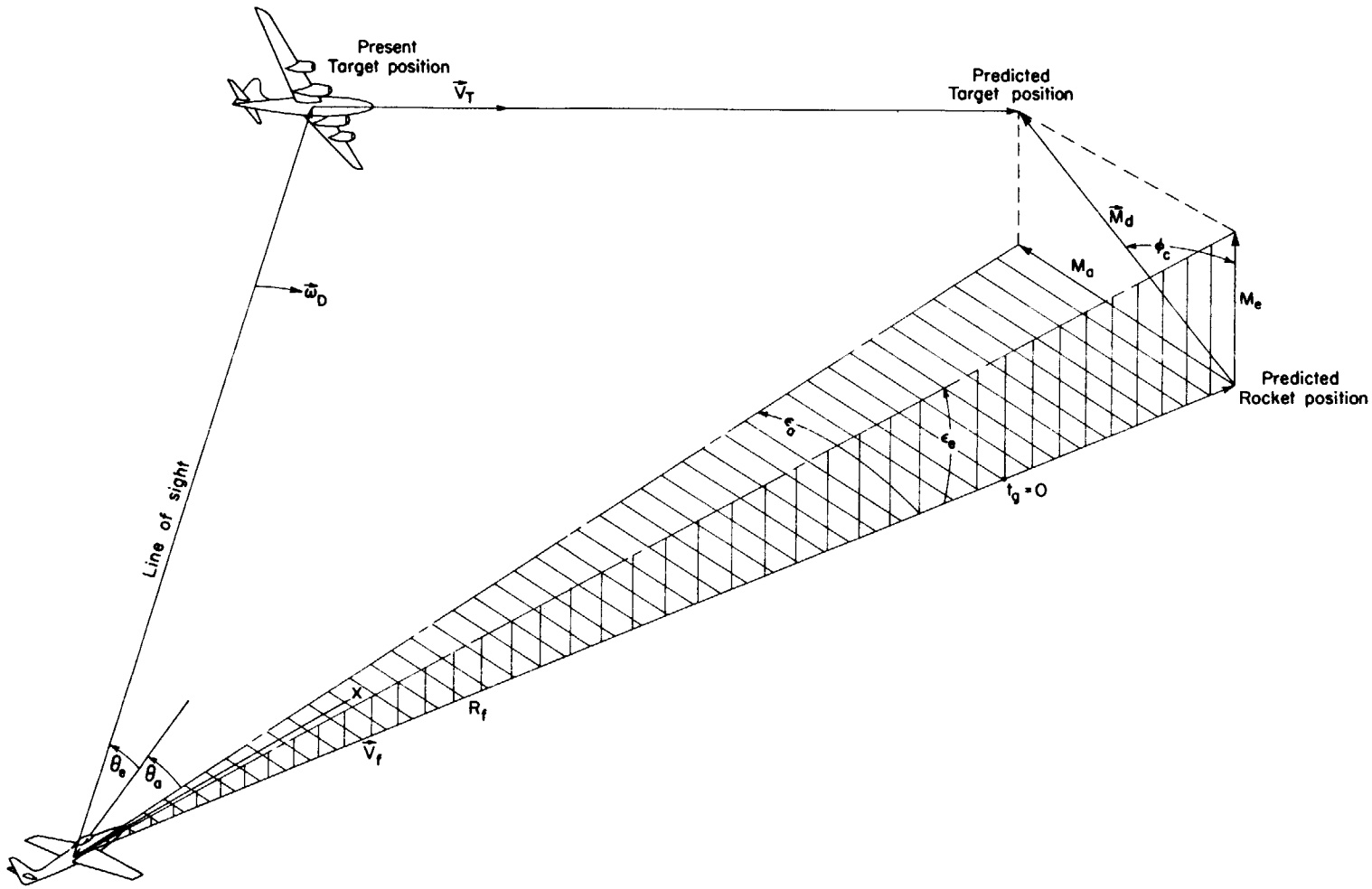

Figure 2.- Geometry used in the study of the automatically controlled interceptor attack run.

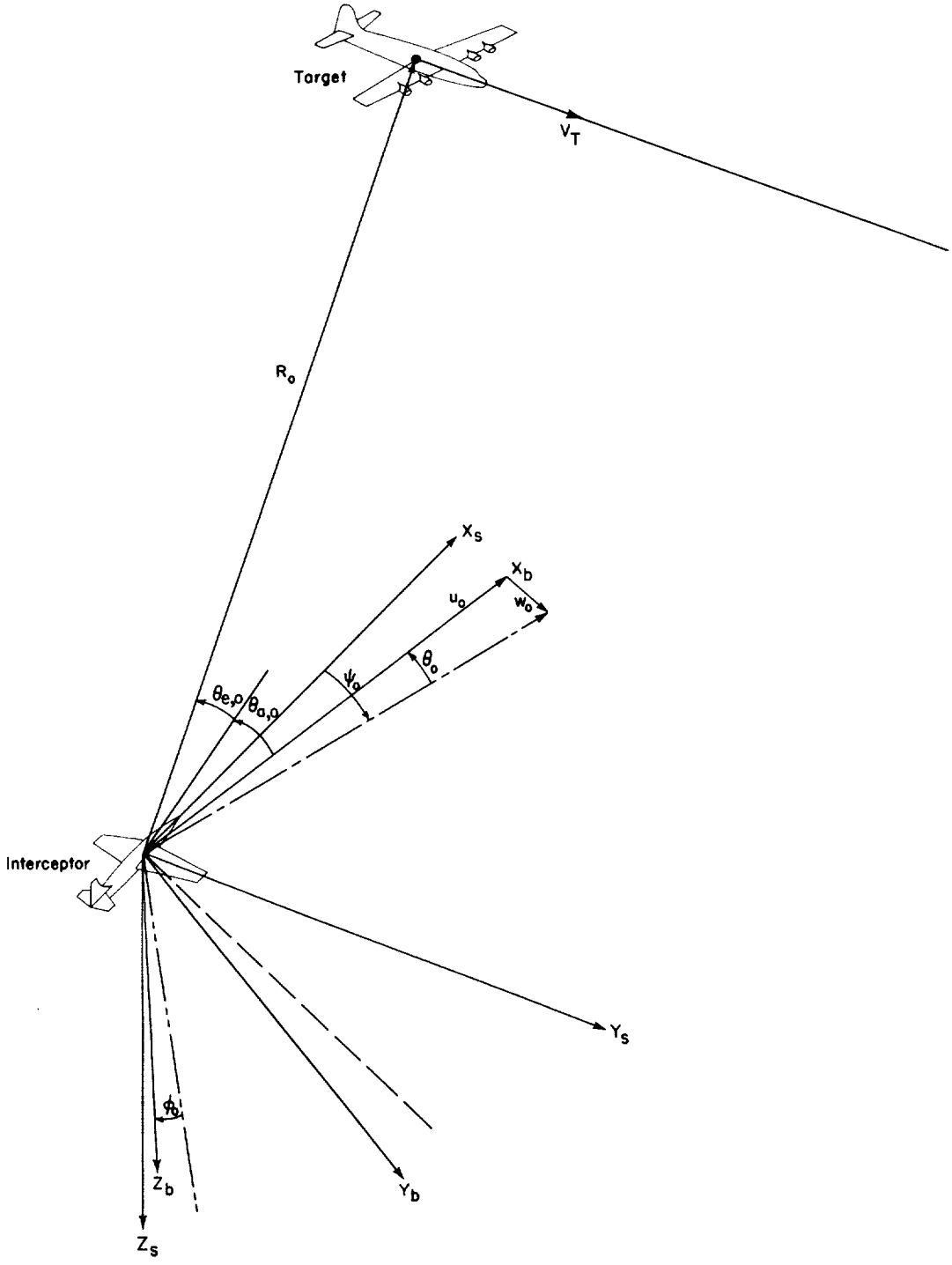

Figure 3.- Axes systems used in the study and interceptor-target orientation.

L-1518

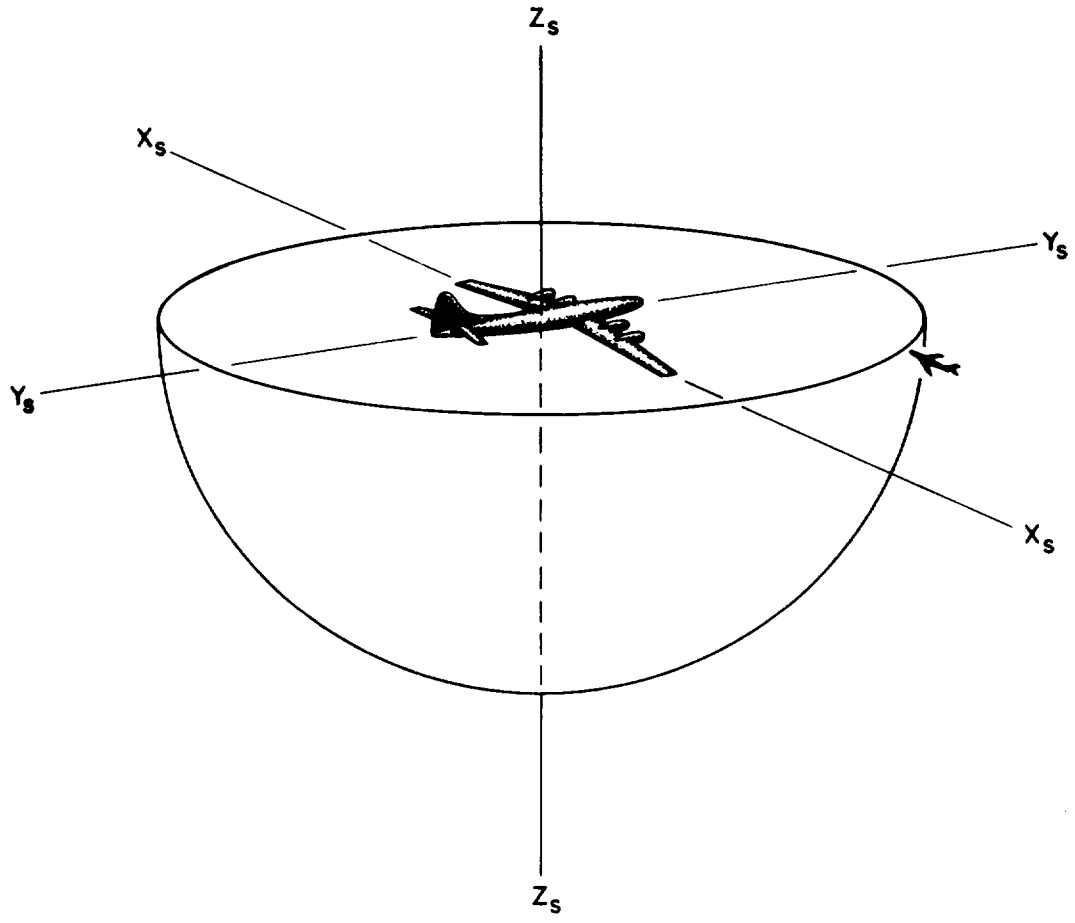

Figure 4.- Pictorial presentation of the interceptor and target orientation.

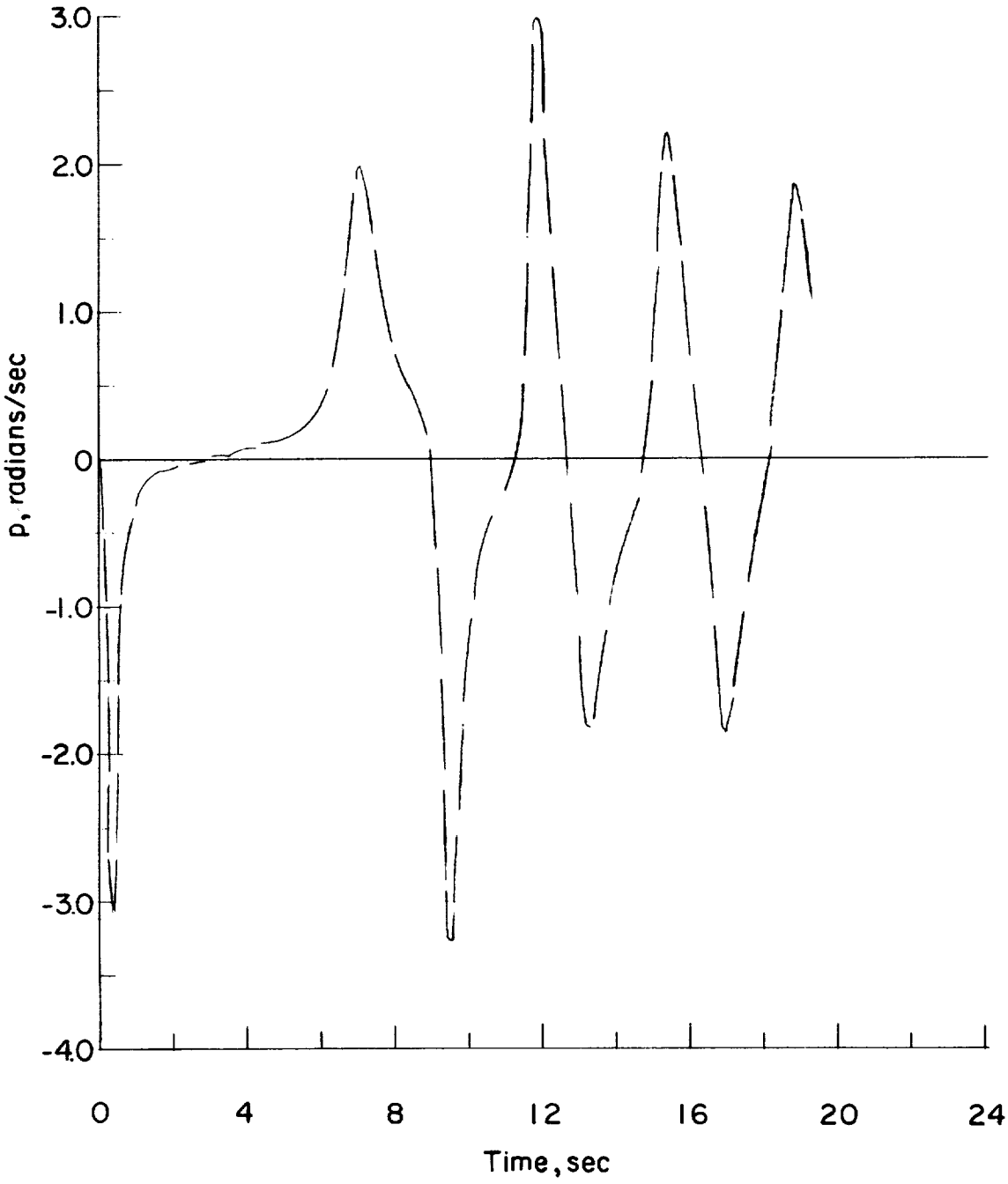

(a) Rolling velocity.

Figure 5.- Time history of the roll response of the automatic interceptor.

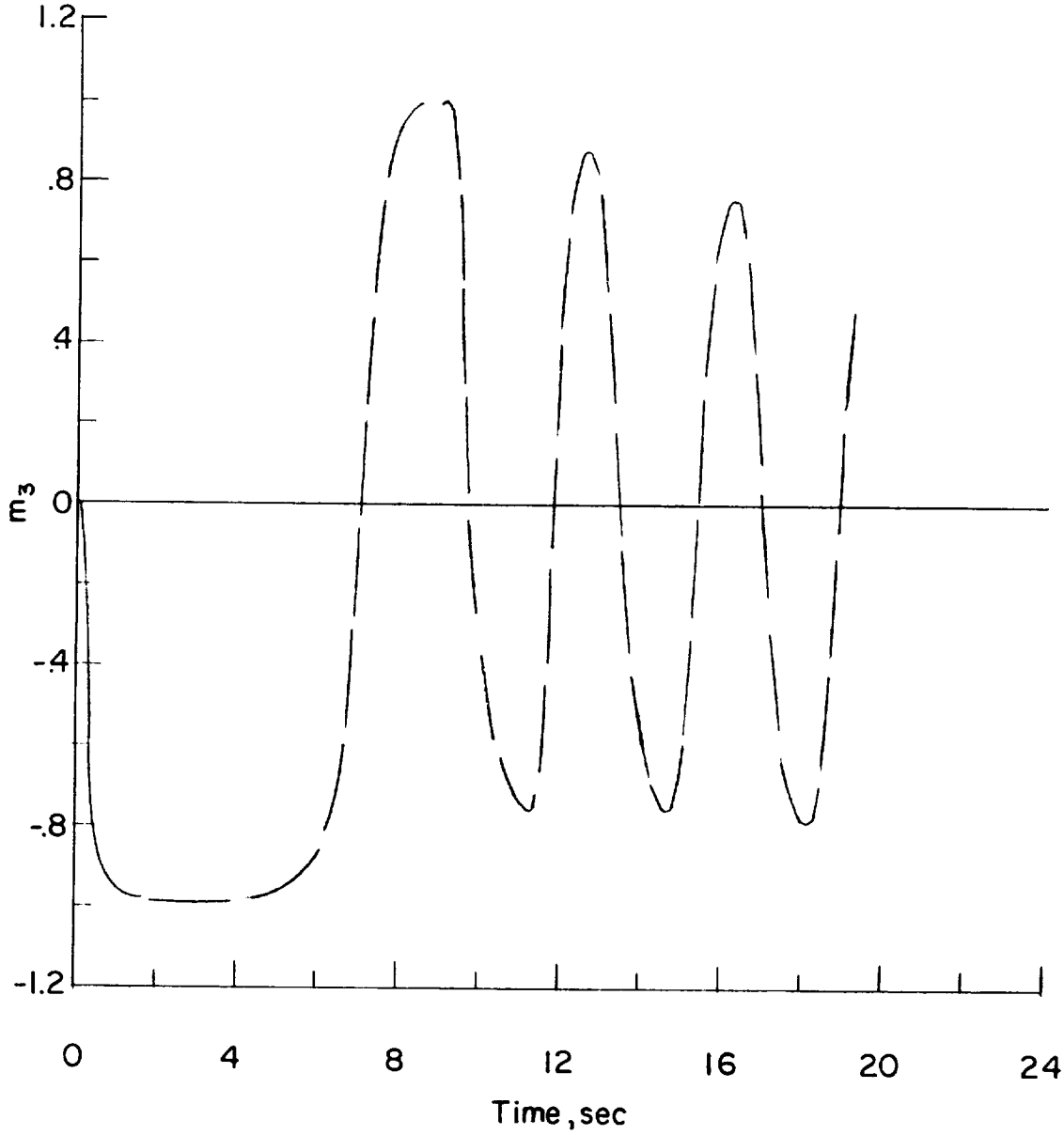

(b) Direction cosine m_3.

Figure 5.- Concluded.

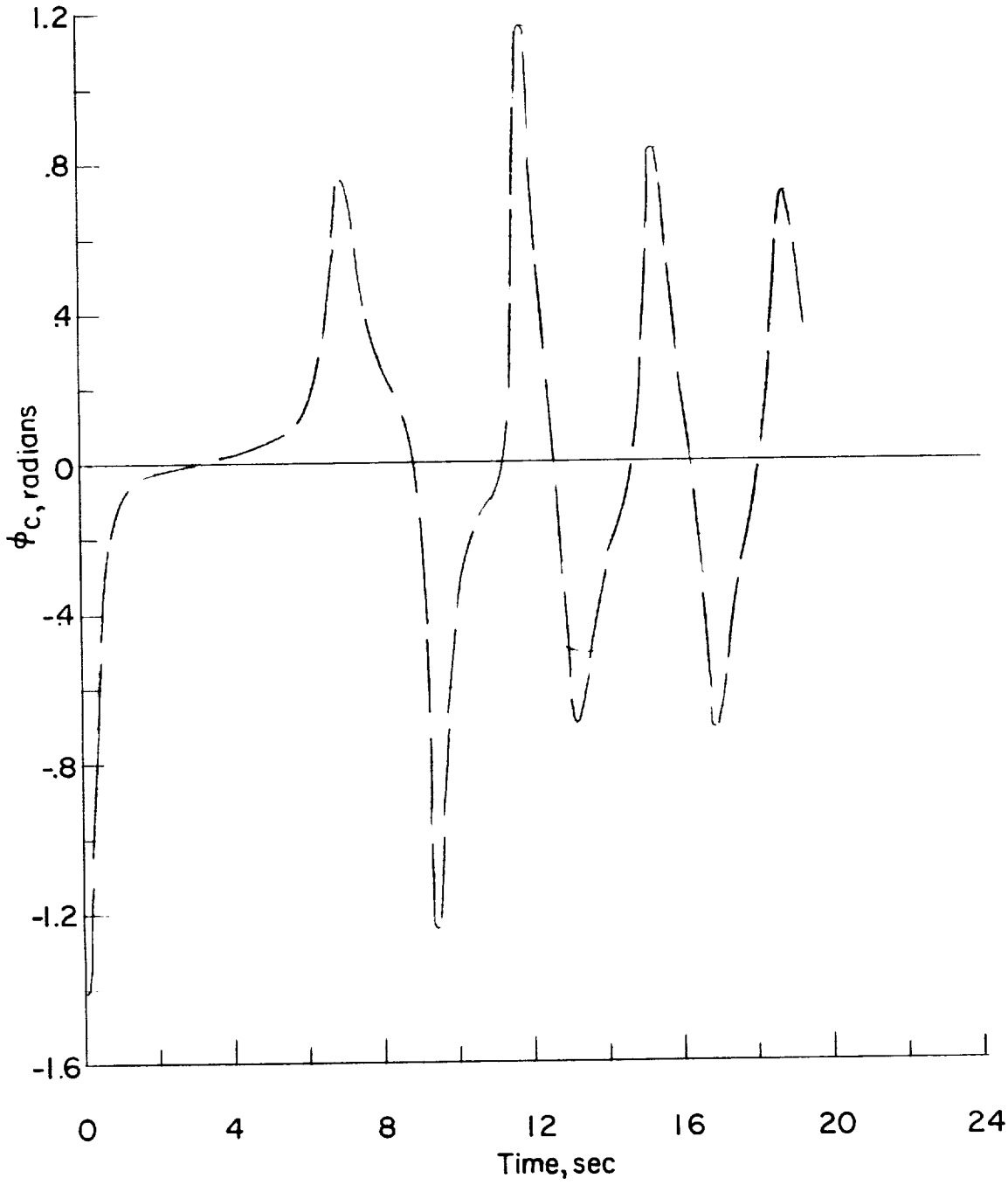

(a) Bank-angle command.

Figure 6.- Time histories of the steering errors for the basic interceptor system.

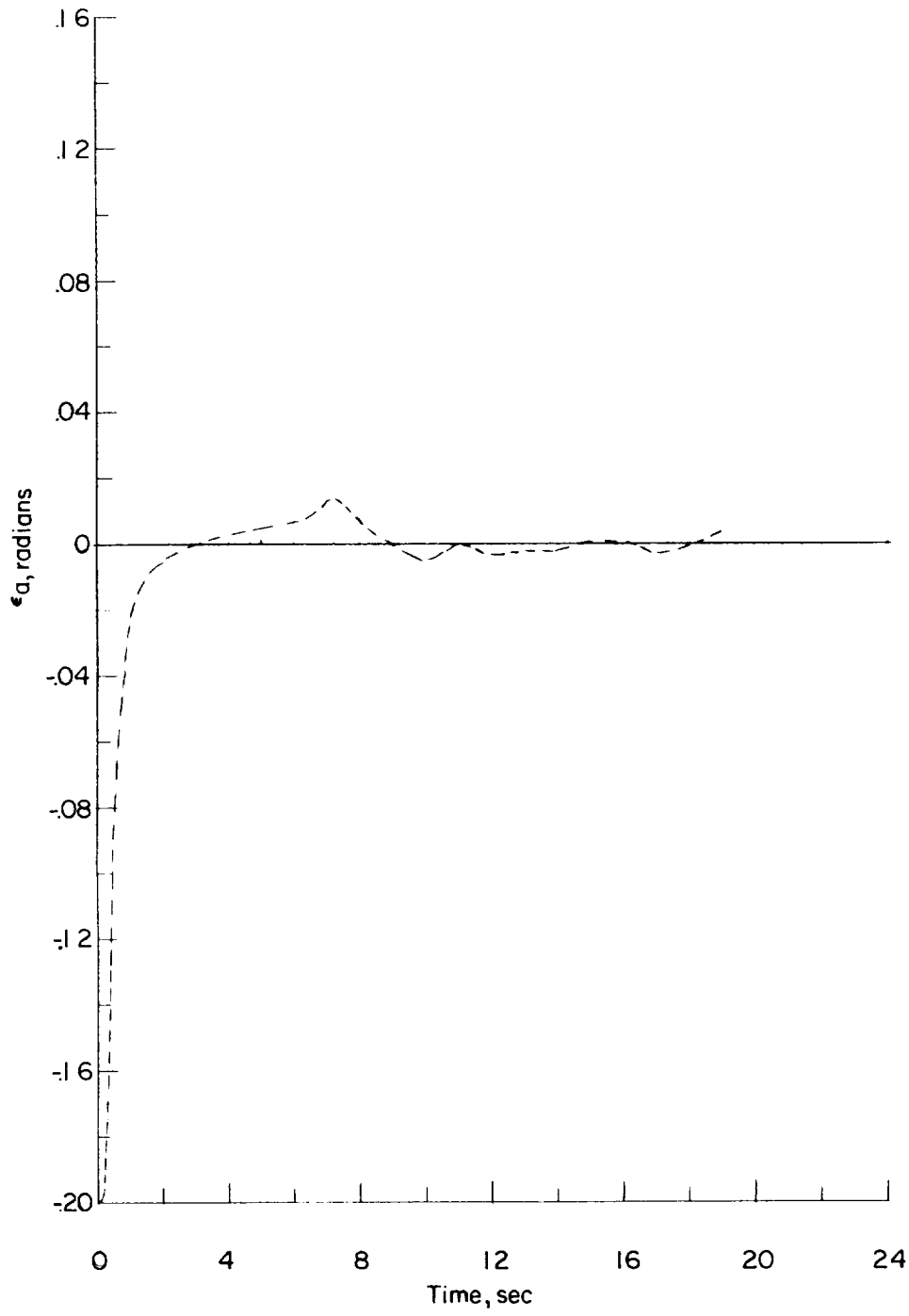

(b) Azimuth steering error.

Figure 6.- Continued.

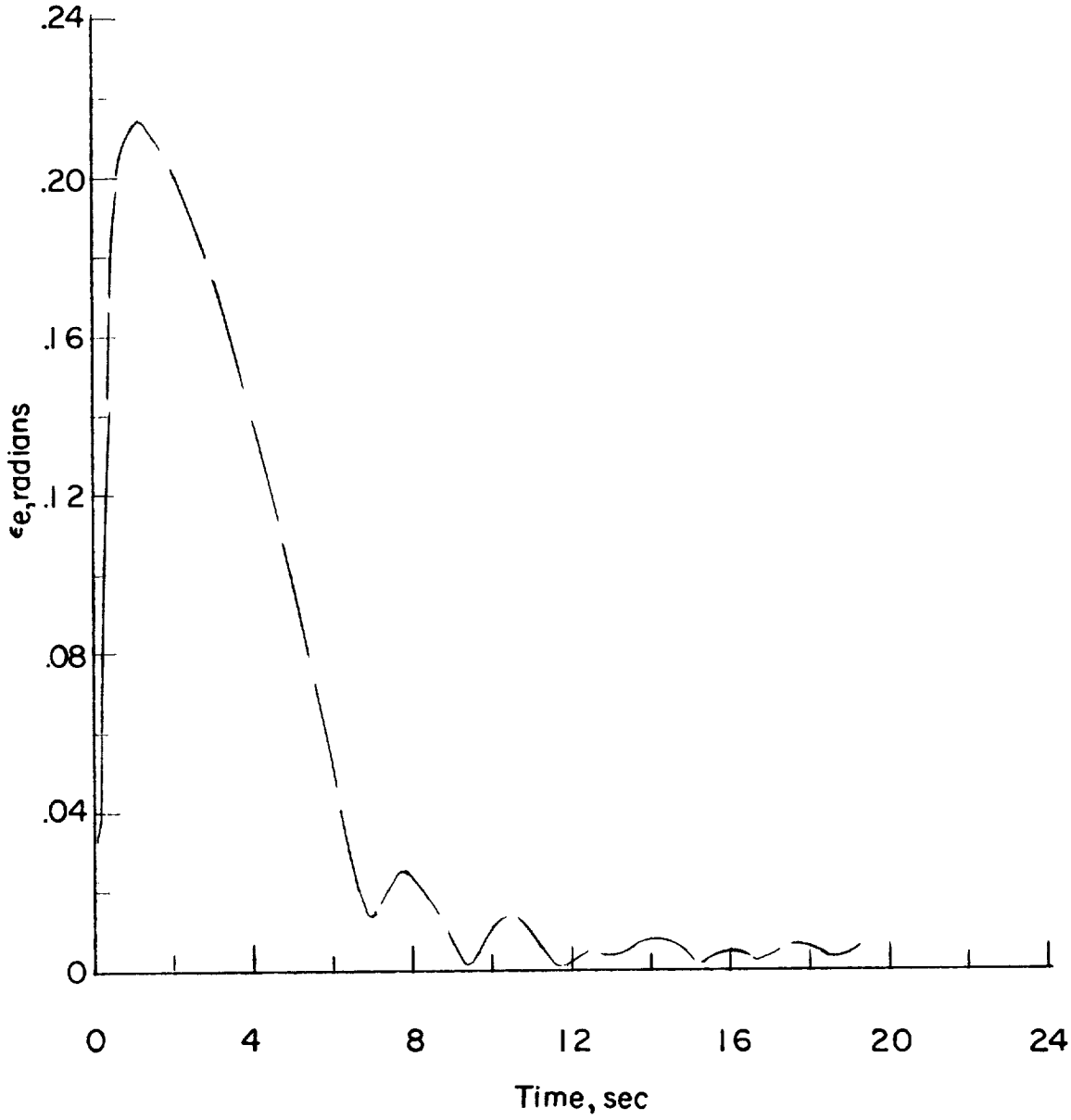

(c) Elevation steering error.

Figure 6.- Concluded.

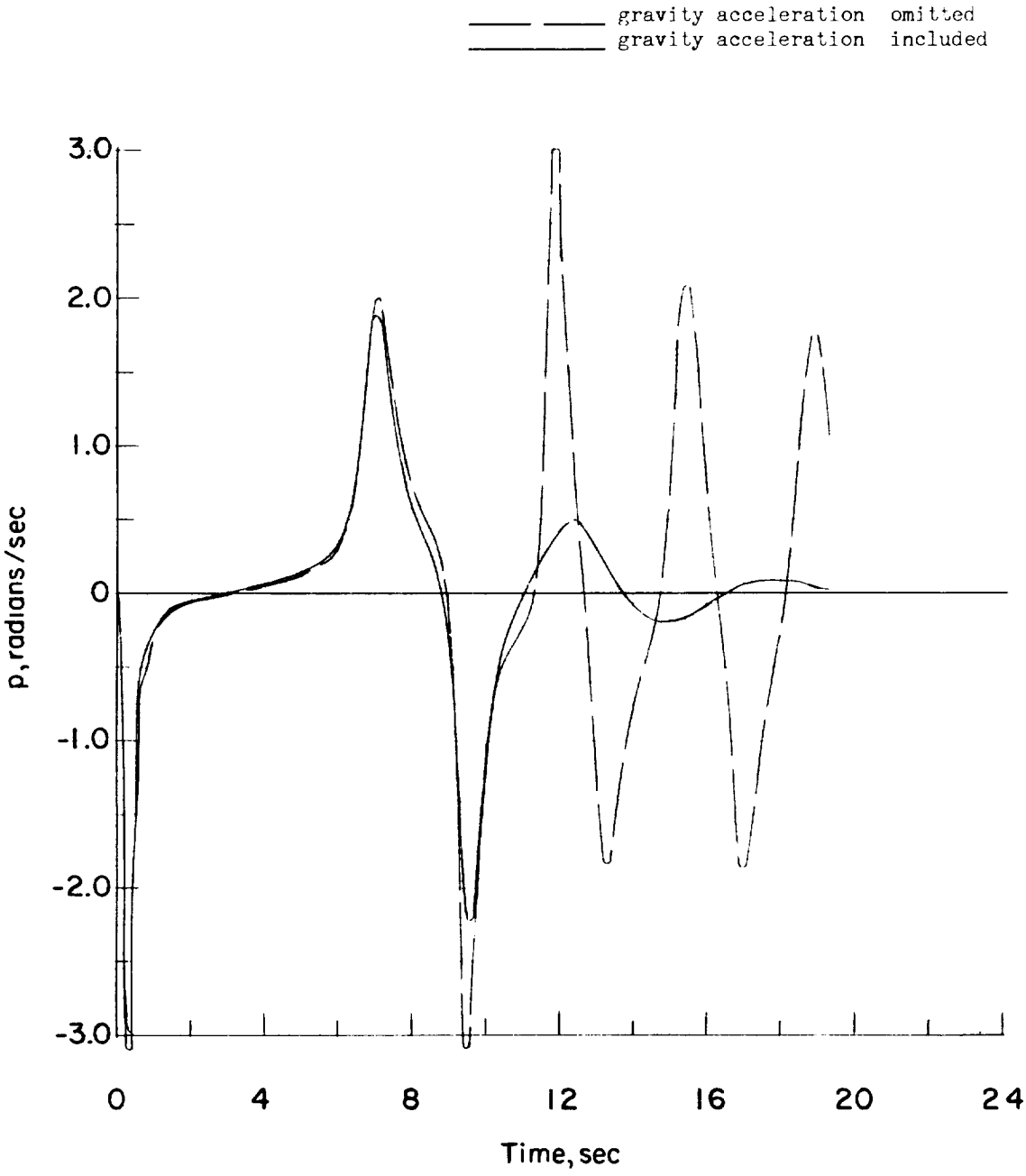

(a) Rolling velocity.

Figure 7.- Time histories of the response of the interceptor showing the effect of including gravity accelerations in the roll command. Nonmaneuvering target.

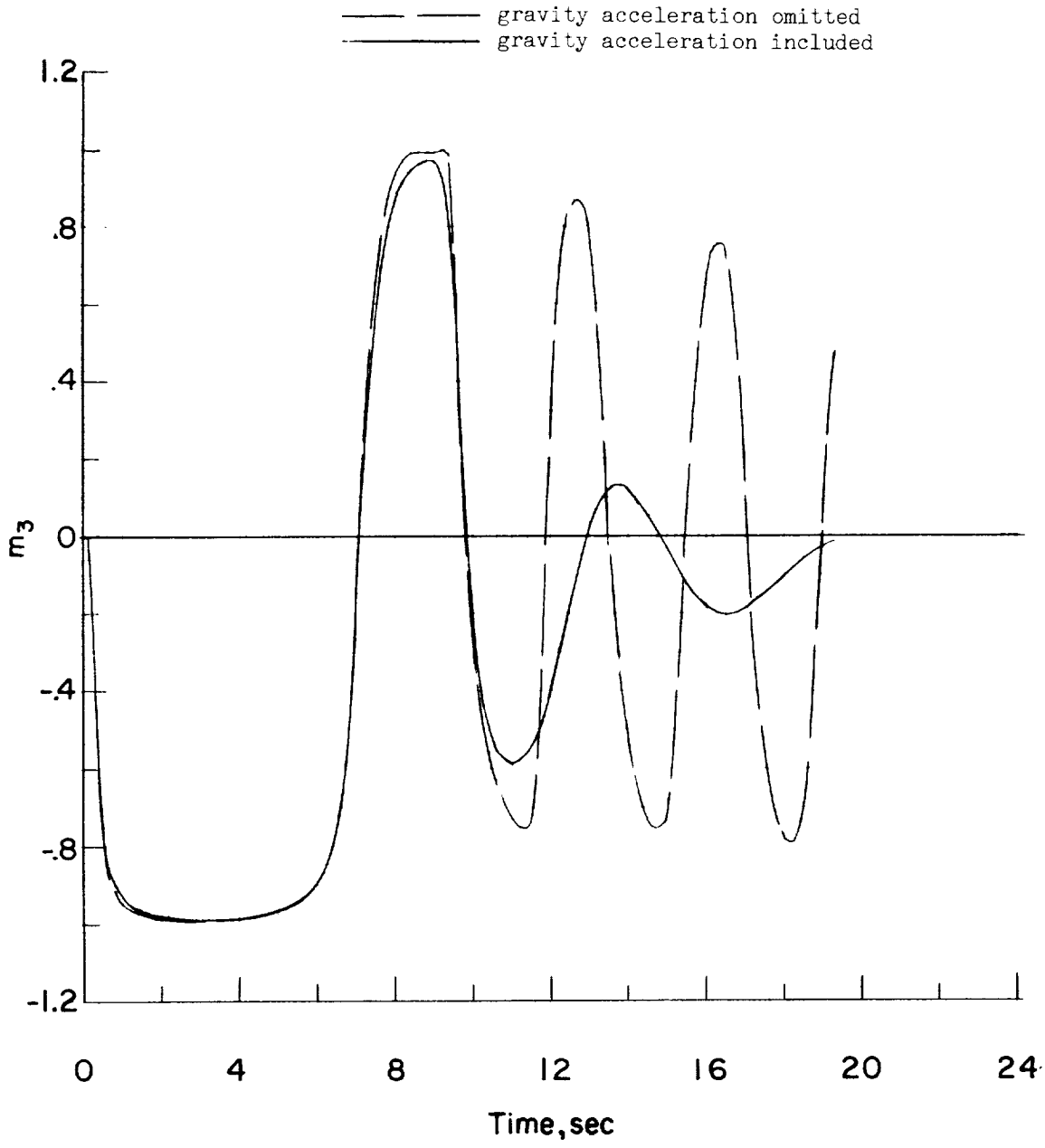

(b) Direction cosine m_3.

Figure 7.- Continued.

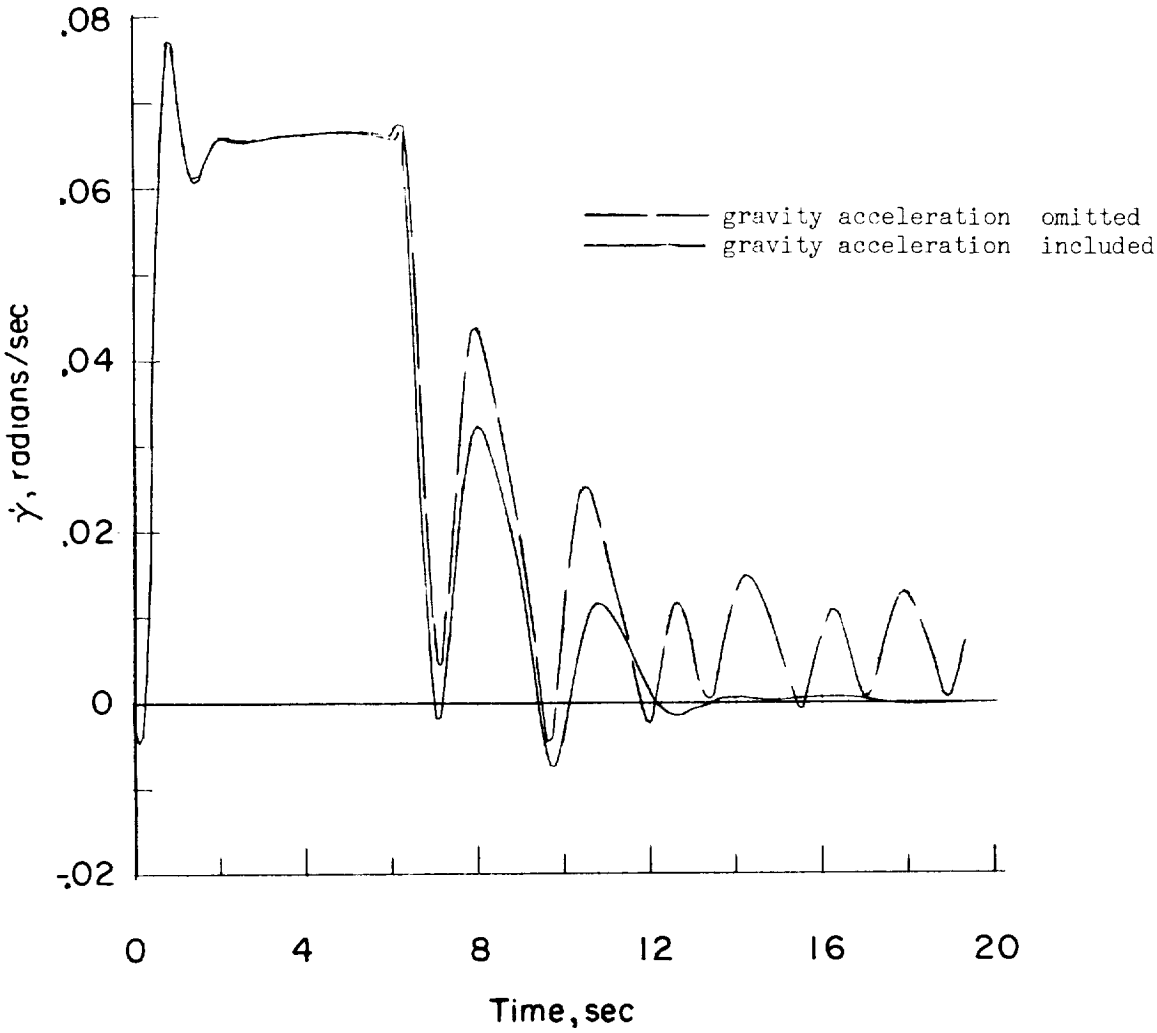

(c) Rate of change of flight-path angle.

Figure 7.- Concluded.

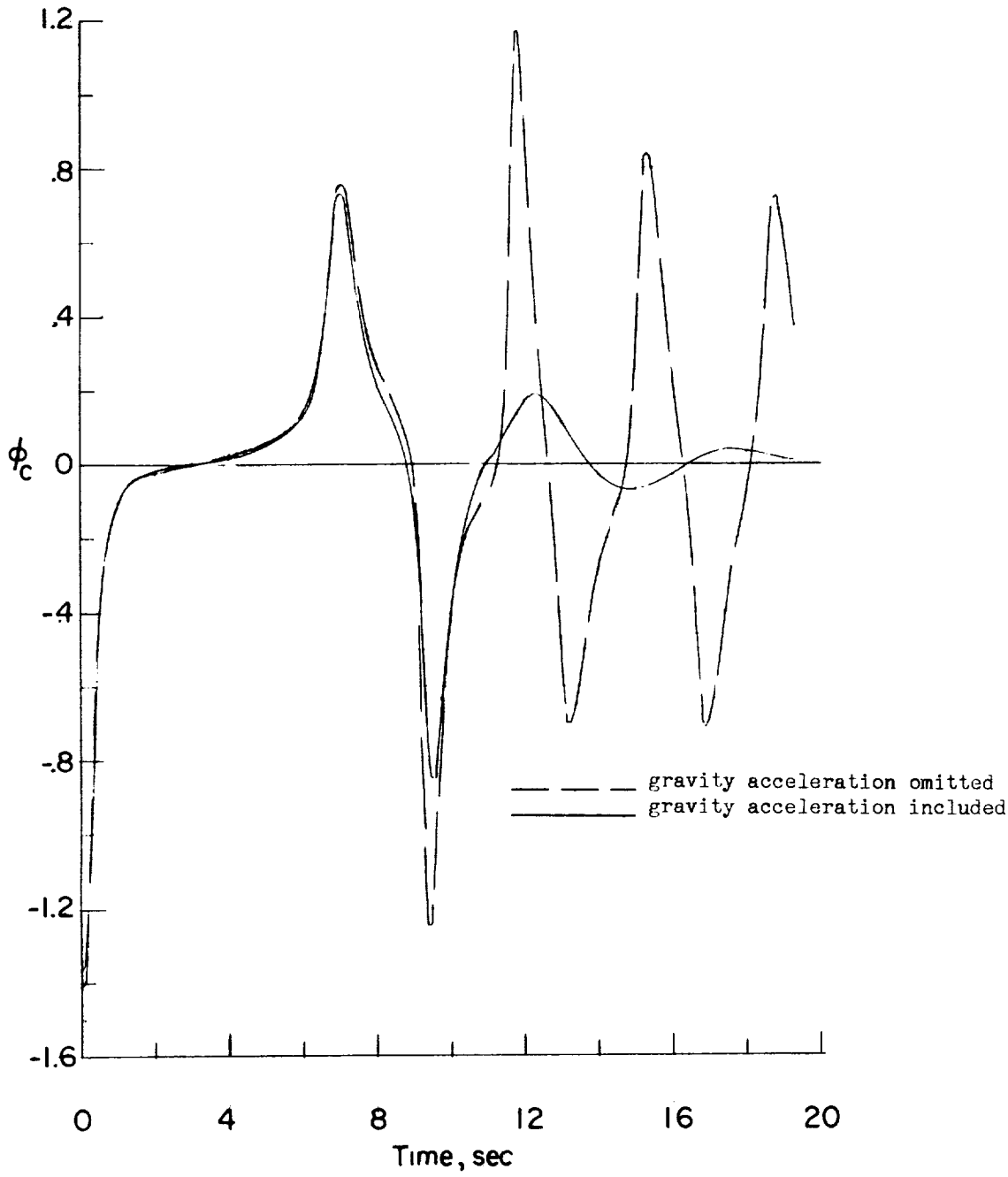

Figure 8.- Time histories of the roll command showing the effect of including the effect of gravity acceleration in roll-command computation. Nonmaneuvering target.

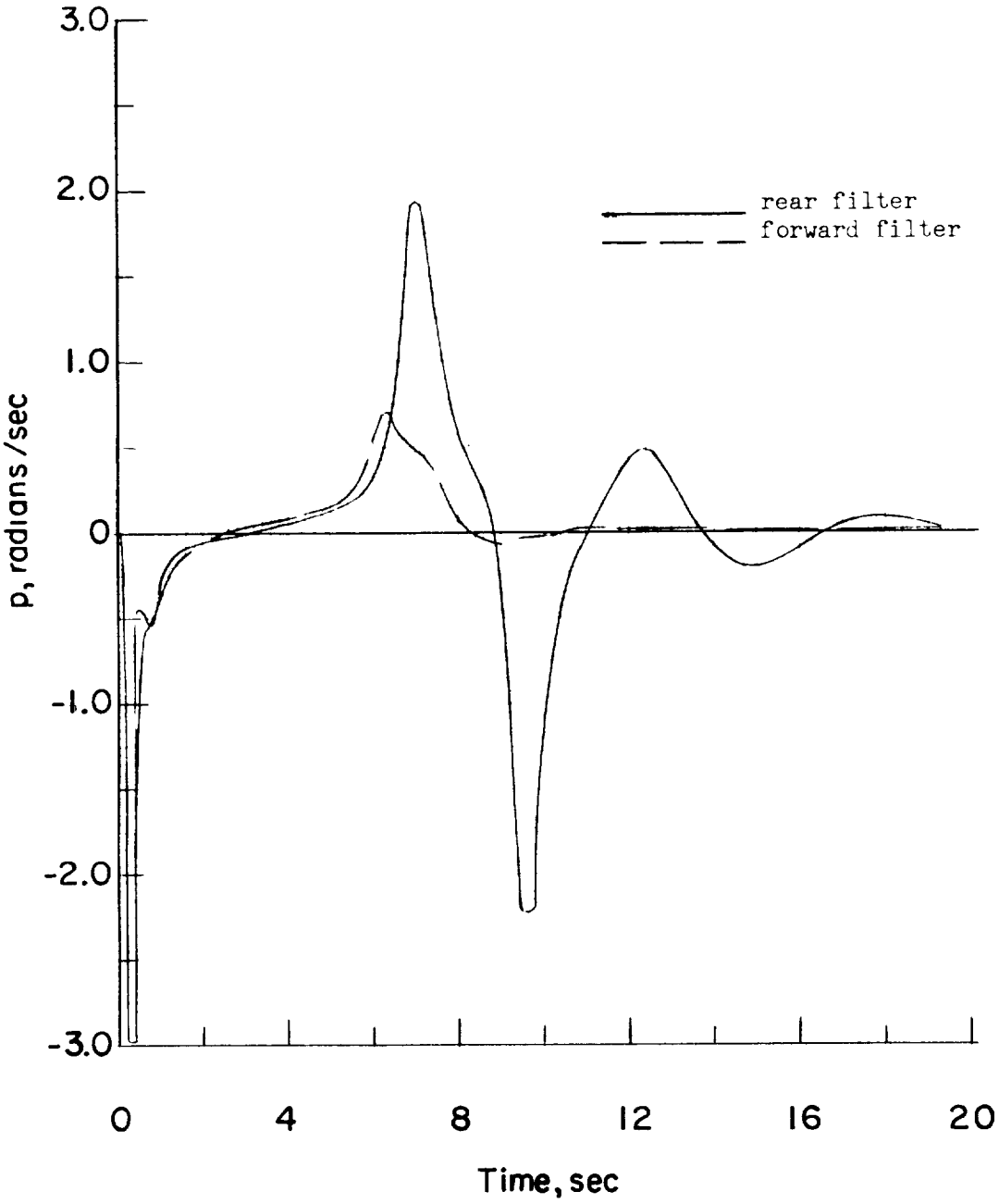

(a) Rolling velocity.

Figure 9.- Time histories of interceptor response showing the effect of changing rear-filter location when gravity accelerations are included in the command computation.

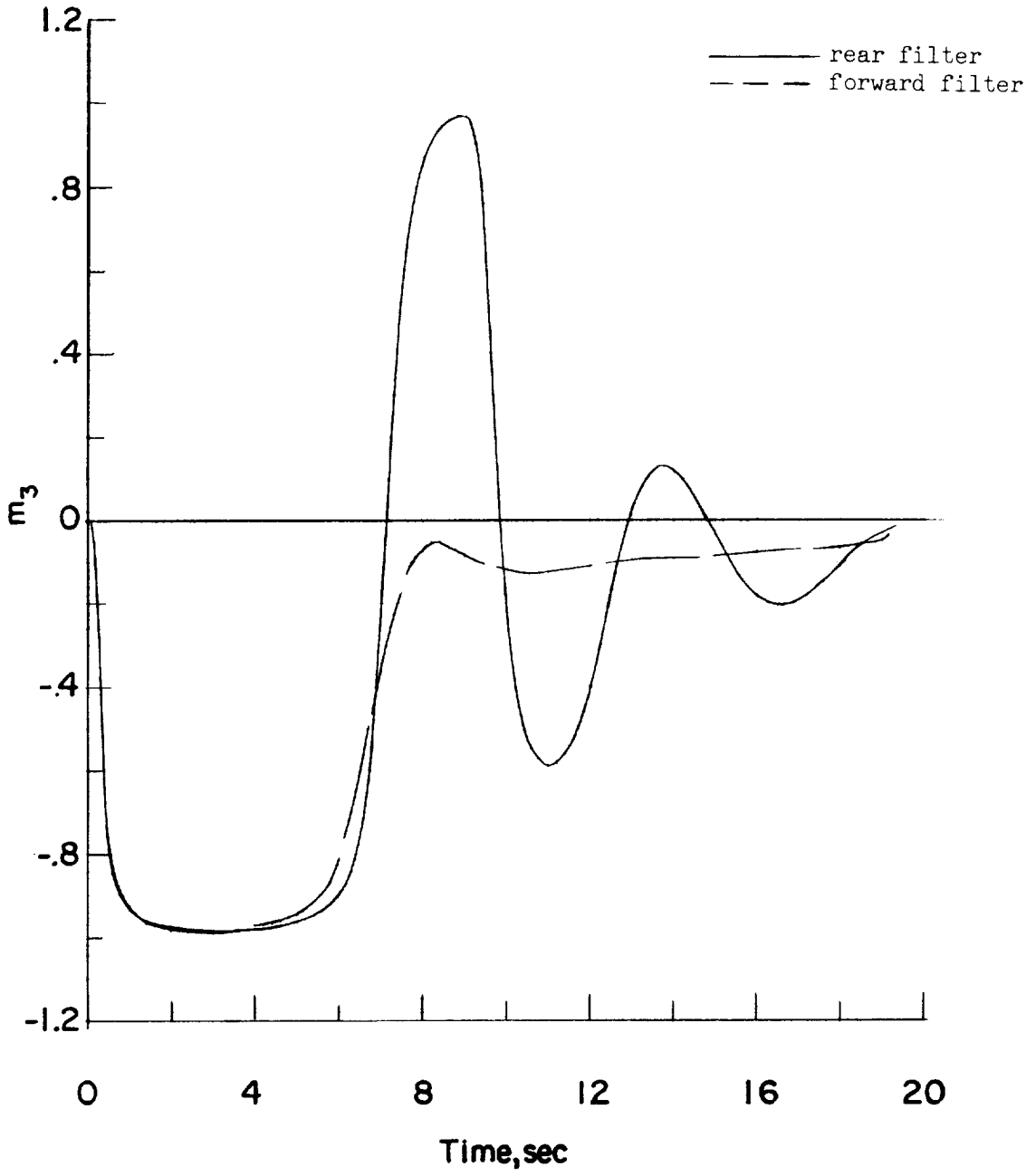

(b) Direction cosine m_3.

Figure 9.- Continued.

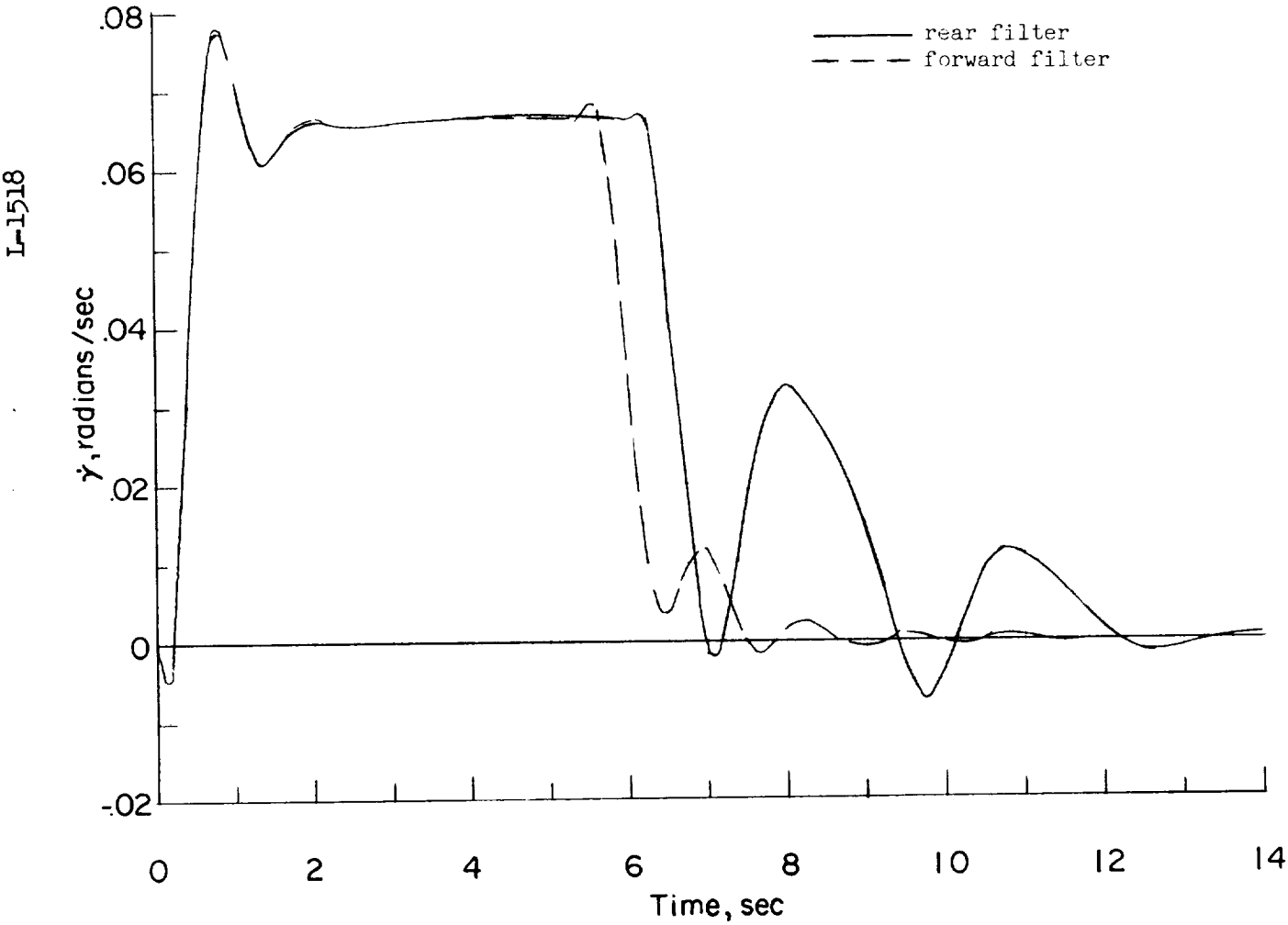

(c) Rate of change of flight-path angle.

Figure 9.- Concluded.

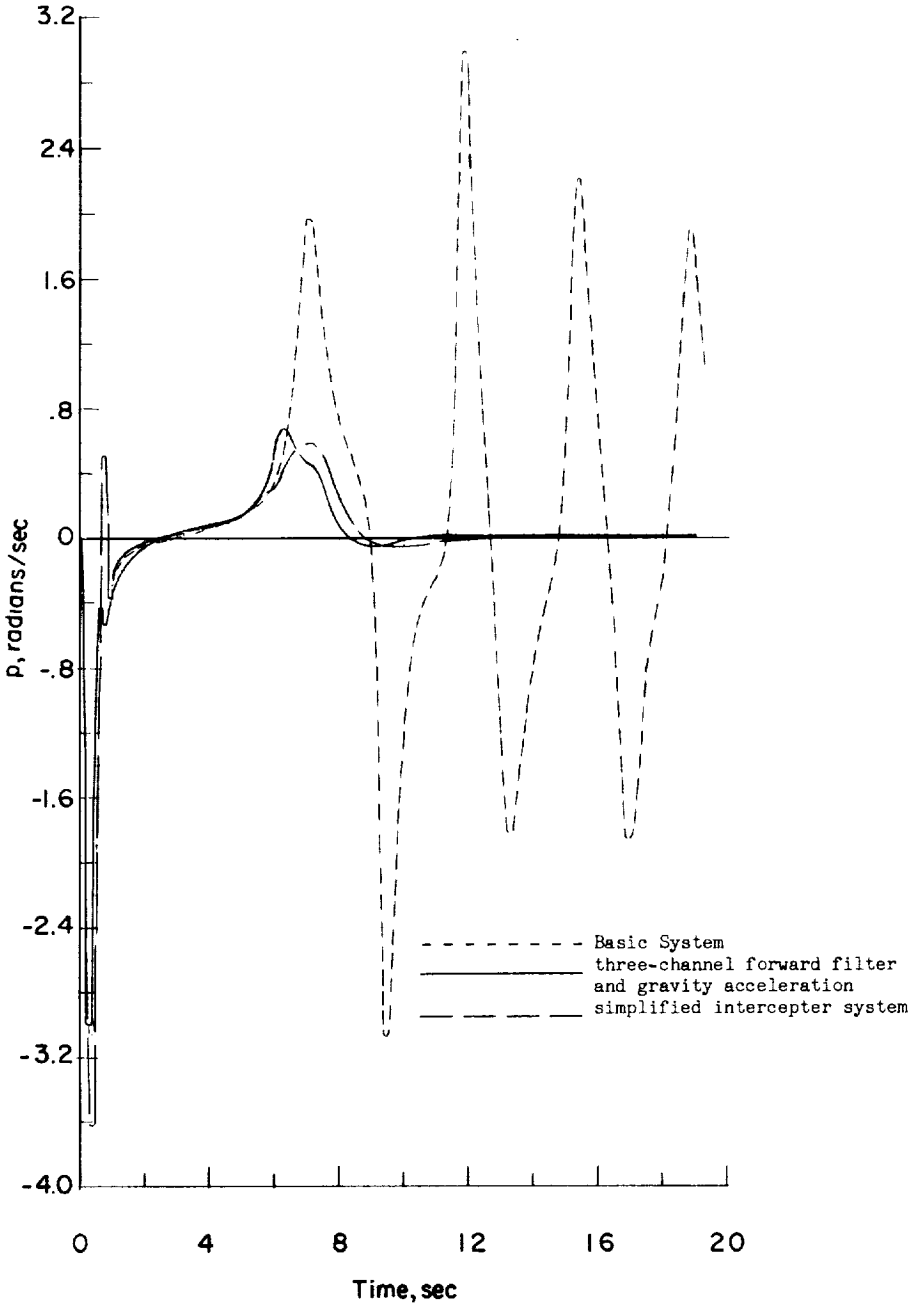

(a) Rolling velocity.

Figure 10.- Time histories of the interceptor response for the basic system, the system with gravity accelerations included in the commands and the three-channel forward filter, and the simplified interceptor command computing and filtering.

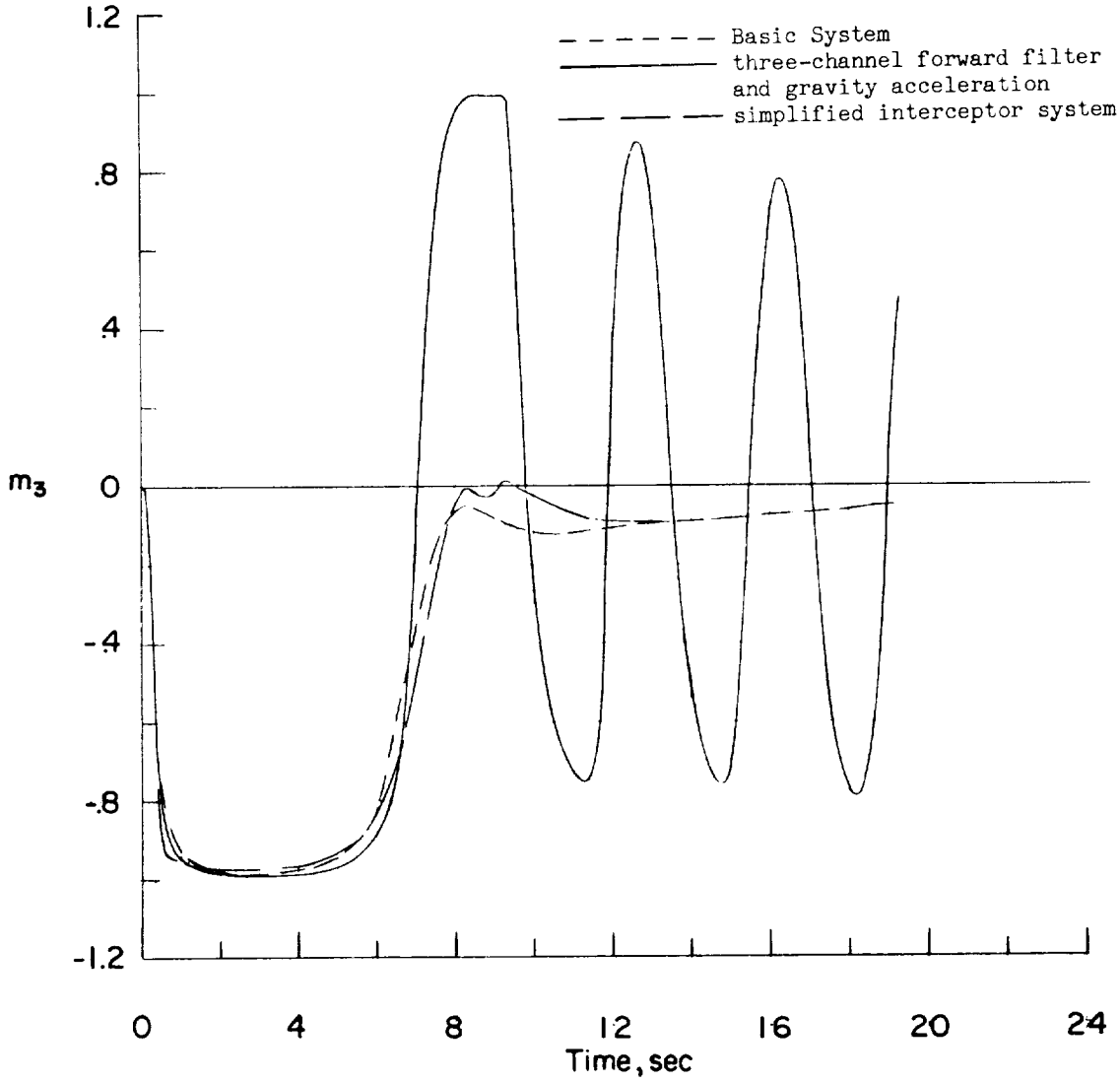

(b) Direction cosine m_3.

Figure 10.- Continued.

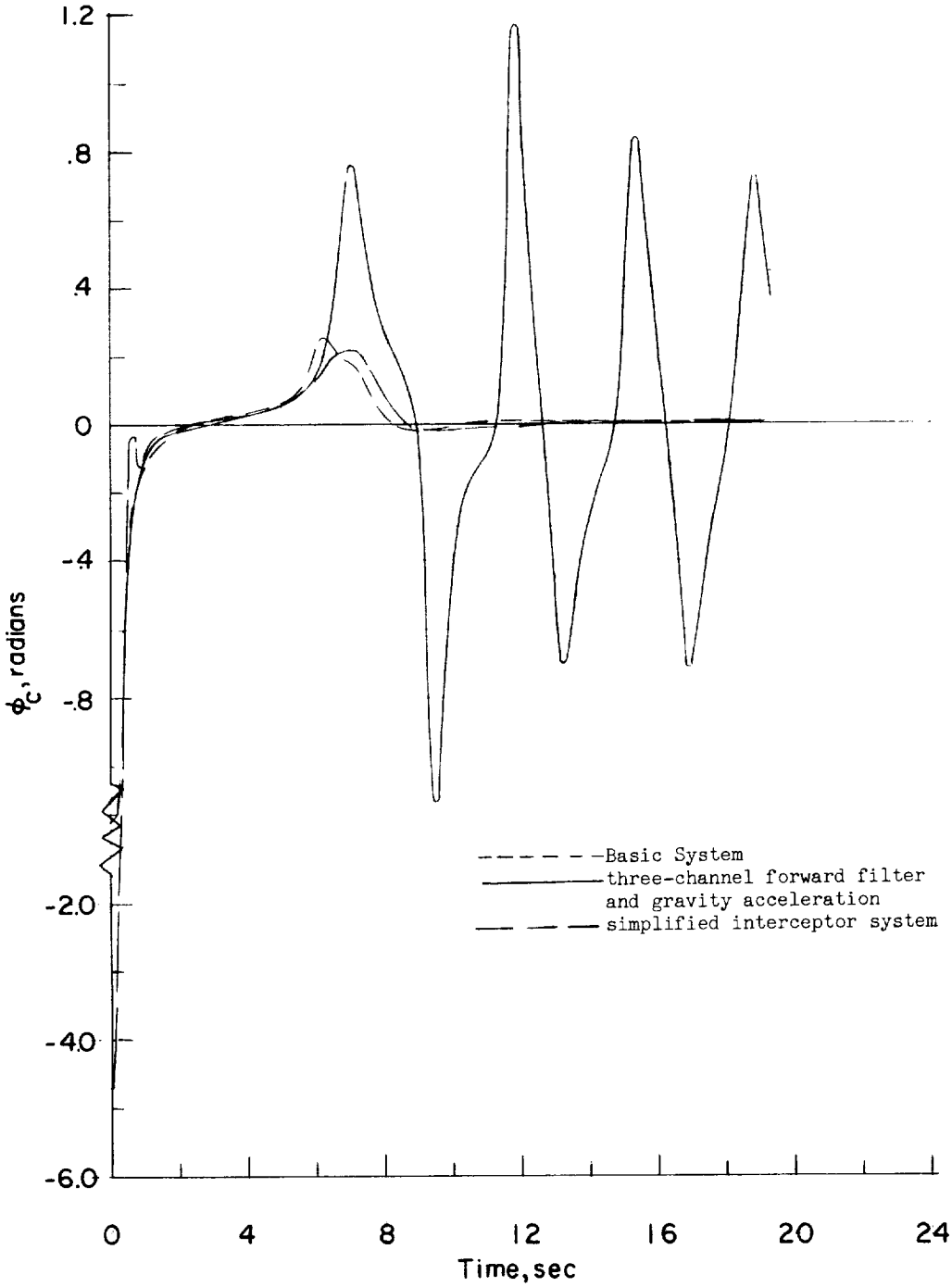

(c) Bank-angle command.

Figure 10.- Continued.

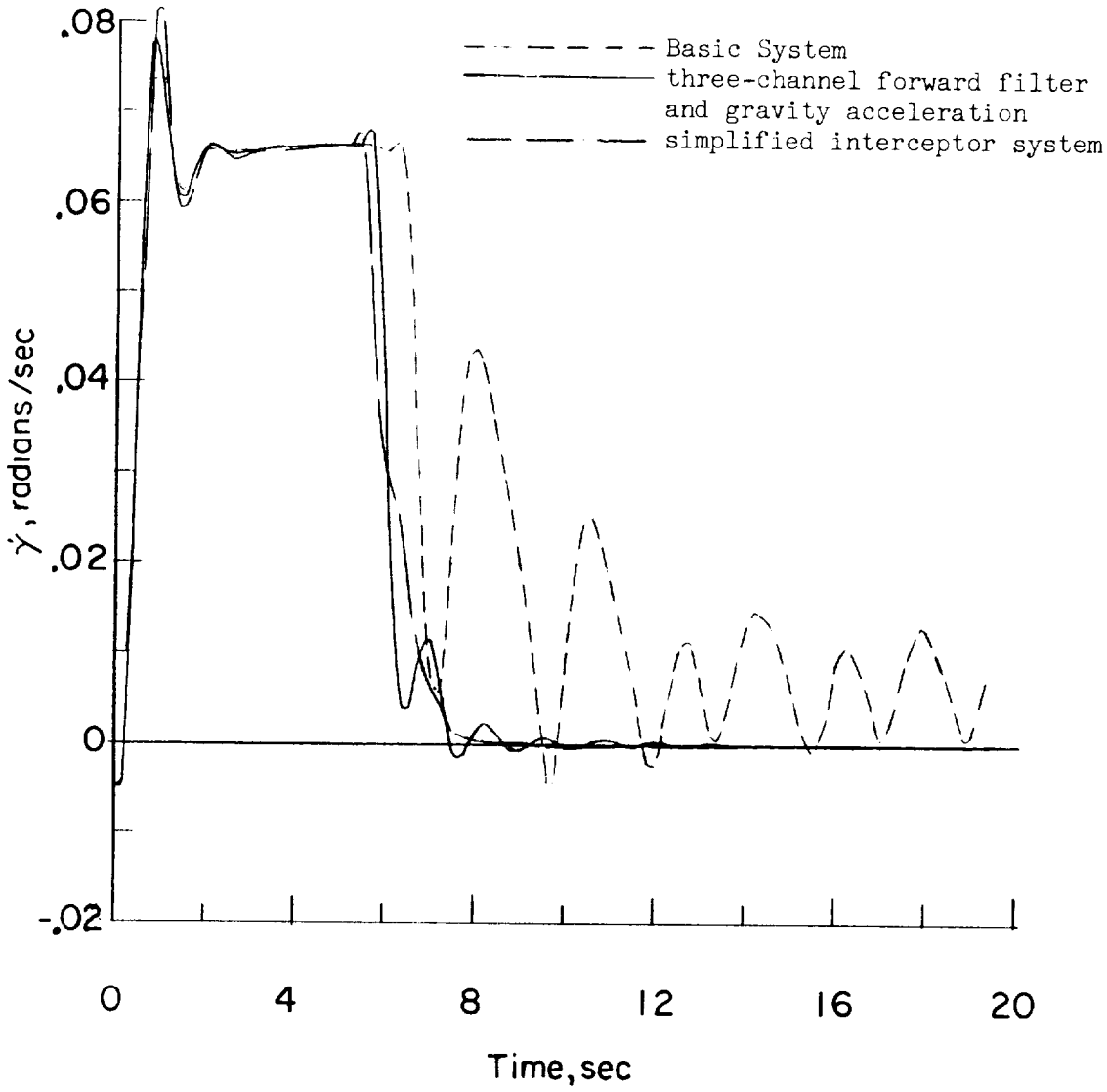

(d) Rate of change of flight-path angle.

Figure 10.- Continued.

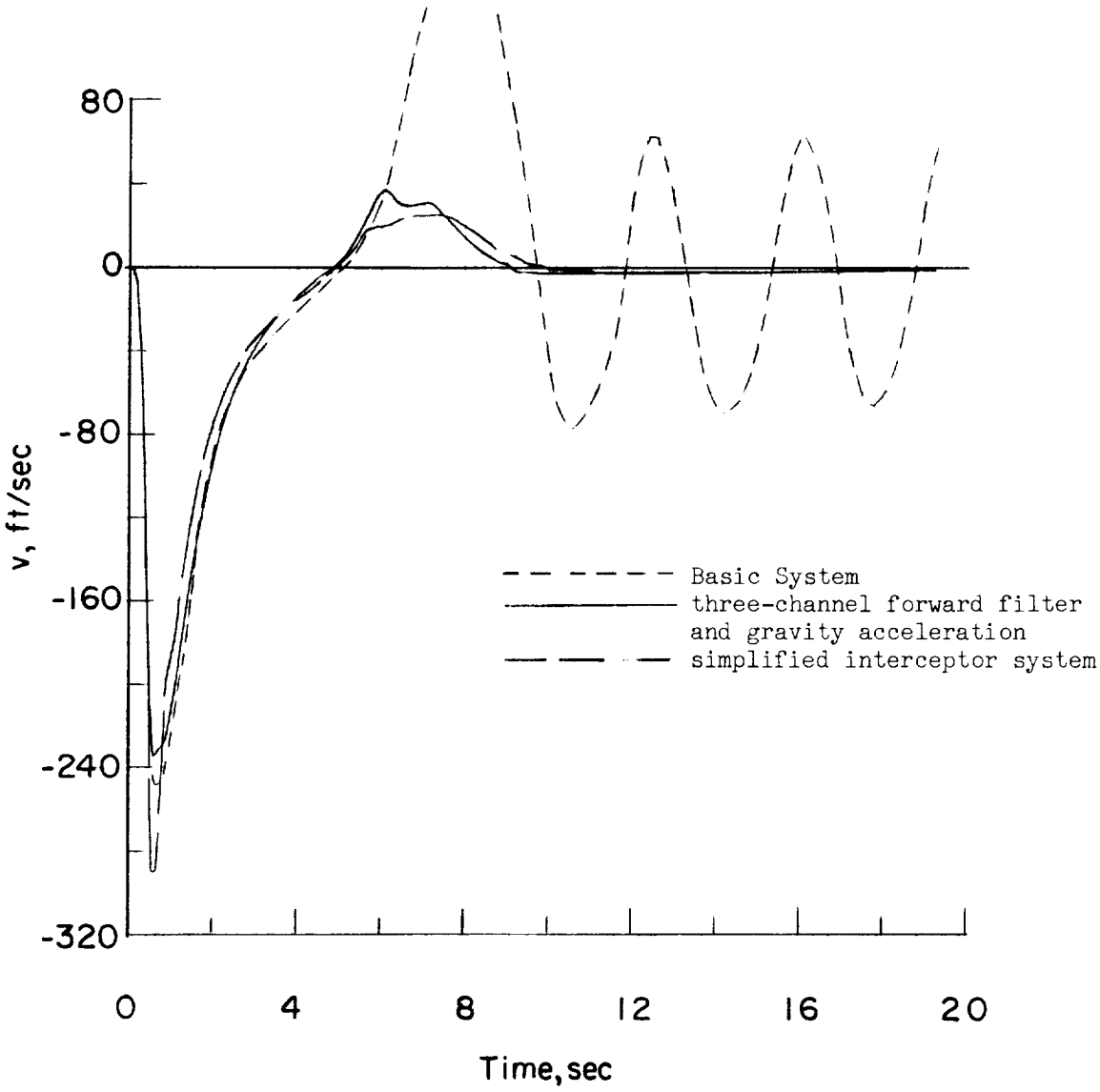

(e) Sideslip velocity.

Figure 10.- Continued.

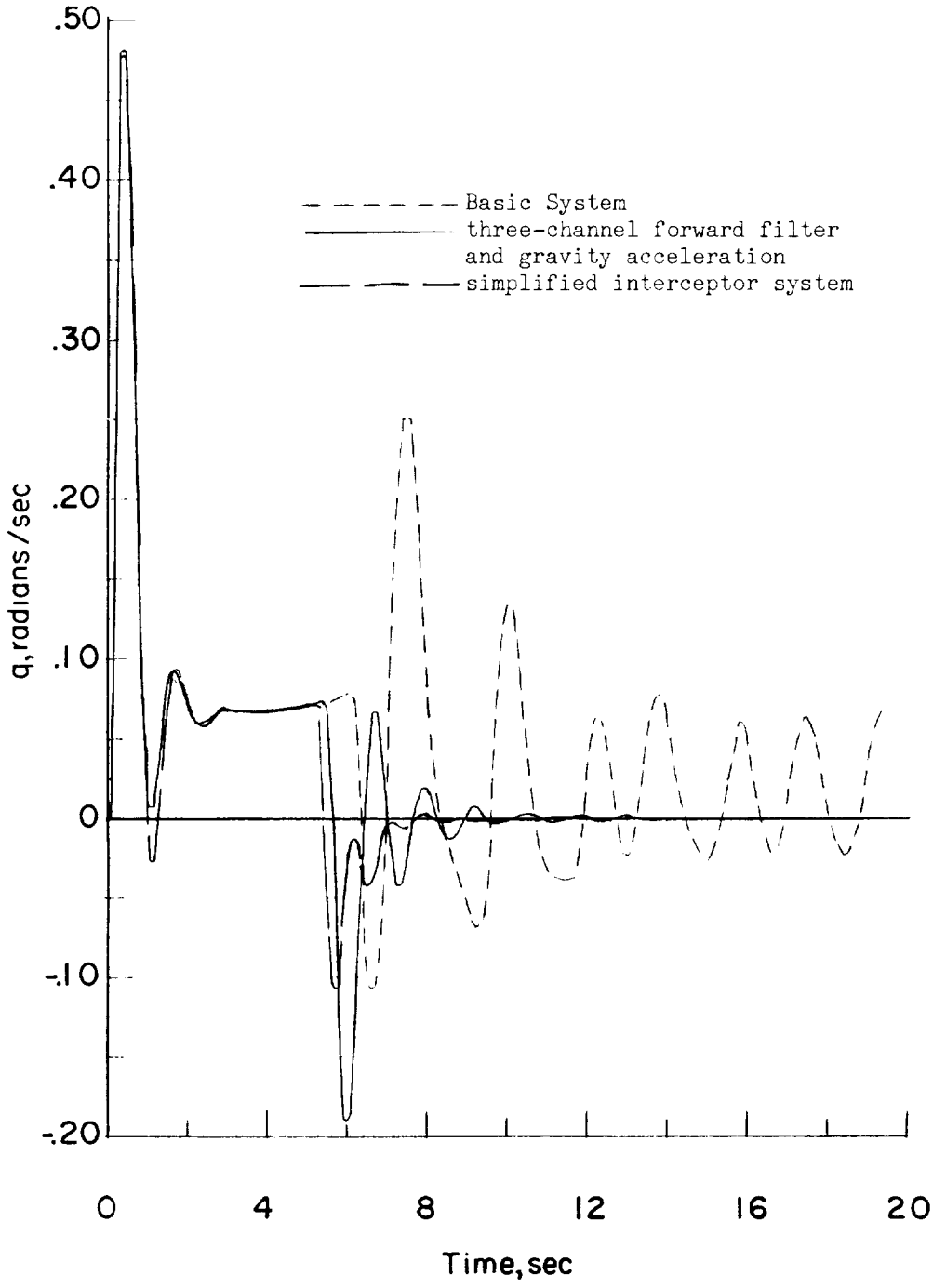

(f) Pitching velocity.

Figure 10.- Continued.

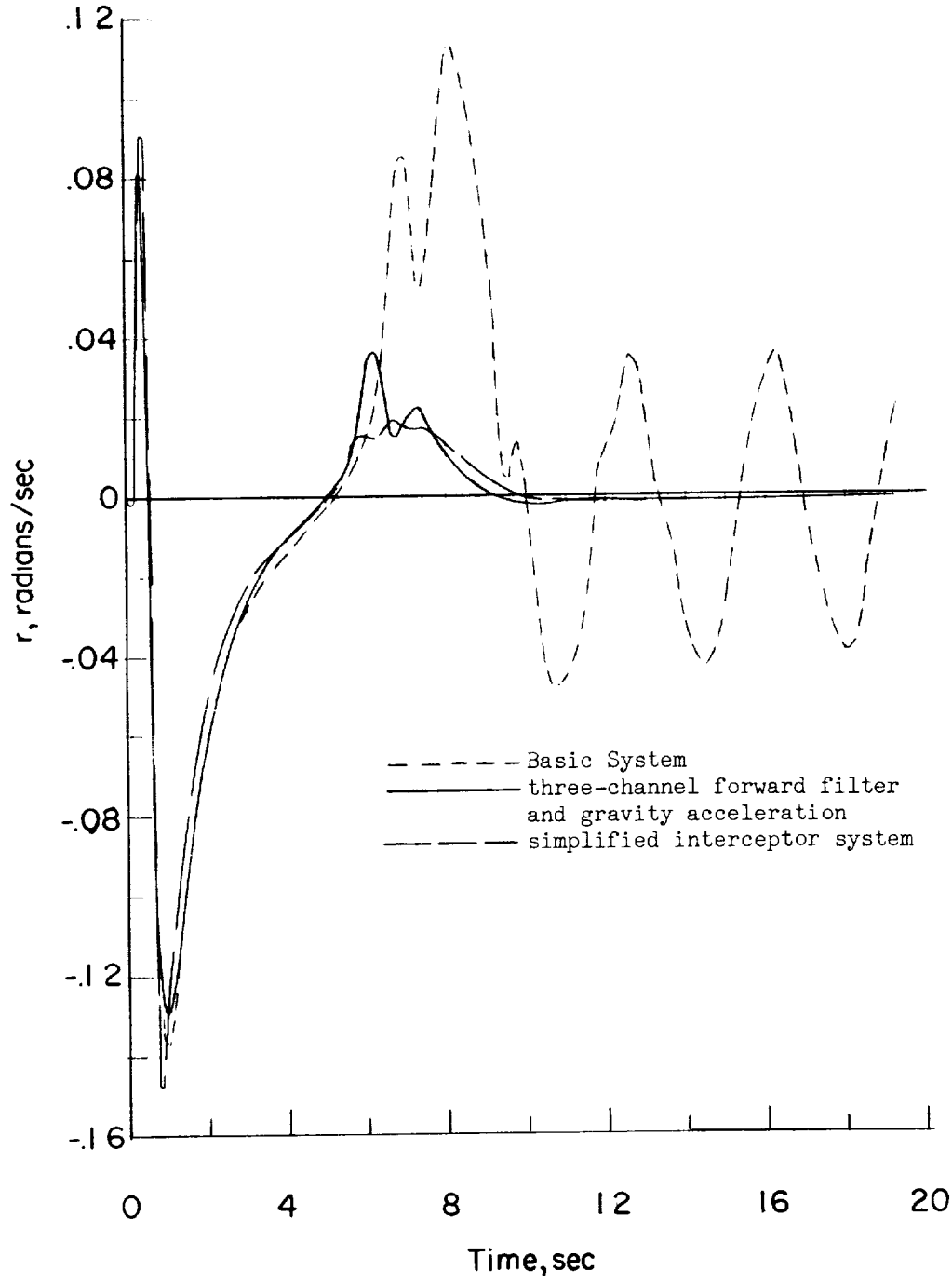

(g) Yawing velocity.

Figure 10.- Concluded.

NASA-Langley, 1962 L-1518

L-1518